IJCRT.ORG ISSN : 2320-2882

INTERNATIONAL JOURNAL OF CREATIVE RESEARCH THOUGHTS (IJCRT)

An International Open Access, Peer-reviewed, Refereed Journal

A Dinitrophenyl-Substituted Pyrrolo[2,3-B]Pyridine Schiff Base: Synthesis, Spectroscopy, And DFT Study

Shikha Kumari

Department of Chemistry, J.M.D.P.L. Mahila College, Madhubani, Bihar 847211, India

Abstract

In this work, we report the synthesis of the Schiff base compound, (Z)-3-((2-(2,4-dinitrophenyl)hydrazono)methyl)-4-methyl-1H-pyrrolo[2,3-b]pyridine, through the condensation reaction between 4-methyl-1H-pyrrolo[2,3-b]pyridine-3-carbaldehyde and (2,4-dinitrophenyl)hydrazine. Elemental analysis, FT-IR, NMR, and UV-Vis spectroscopic measurements confirmed the structural composition of DMP. FT-IR and NMR measurements provided evidence for the formation of a hydrazone linkage with nitro and aromatic functionalities. The UV-Vis and DFT results revealed a clear signature of intramolecular charge transfer with an estimated HOMO-LUMO energy gap of 3.125 eV, which is in close agreement with the experimental absorption at 390 nm. The molecular electrostatic potential (MEP) map displayed distinct positive and negative potential regions indicating the probable reactive sites. These confirm the structural veracity of the synthesized compound with promises for applications in the area of optoelectronics and sensing.

Keywords- dinitrophenyl, elemental, spectroscopy, DFT, HOMO

1. Introduction

Nitrogen-containing heterocyclic compounds remain a cornerstone of medicinal chemistry due to their exceptional reactivity, adjustable physicochemical characteristics, and wide range of biological activities [1,2]. Of these, the pyrrolo[2,3-b]pyridine framework, a fused bicyclic system joining pyrrole and pyridine rings, has emerged as one of the important structural motifs in pharmacophore design exhibiting a variety of biological activities like antitumor, anti-inflammatory, antimicrobial, and enzyme inhibitory activities [3–5]. Strategic substitution in this heterocyclic core allows modulation of its electronic properties and optimization of its affinity for specific biological targets [5–7].

A specific route for the derivatization of such frameworks in a flexible and handy manner is the synthesis of Schiff bases, hydrazone derivatives in particular, which are generally obtained by condensation reactions from hydrazines with carbonyl compounds such as aldehydes or ketones [8–10]. These derivatives are

known for extended π-conjugation, structural rigidity, and efficient electron delocalization [11,12]. The presence of a 2,4-dinitrophenyl group is particularly useful, since its strong electron-withdrawing effect may alter the electronic landscape of the molecule, enhance electrophilicity, and give rise to favorable intermolecular interactions, particularly in biological contexts [13,14].

In this work, we report the synthesis of a novel Schiff base, namely, (Z)-3-((2-(2,4-dinitrophenyl)hydrazono)methyl)-4-methyl-1H-pyrrolo[2,3-b]pyridine, which incorporates the biologically important pyrrolo[2,3-b]pyridine skeleton with the electron-deficient dinitrophenyl hydrazone moiety. The title compound was fully characterized by means of elemental analysis, FT-IR, 1H NMR, and UV–Vis spectroscopy, which verified its composition and the presence of the main functional groups intact.

In order to further support the experimental results and also explore the electronic behavior of the molecule, density functional theory computations at the B3LYP/6-311++G(d,p) level of theory were carried out. The frontier molecular orbital analysis (HOMO-LUMO) explained the electronic transitions and chemical reactivity, and MEP mapping showed the regions of electron density that can act as active sites for molecular interactions.

This experimental and theoretical investigation allows for a detailed correlation between the structural framework and electronic features of the synthesized Schiff base and therefore provides a sound basis for its possible development in biological and material science applications.

2. Materials and Methods

2.1 Materials

All chemicals required for the synthesis of (Z)-3-((2-(2,4-dinitrophenyl)hydrazono)methyl)-4-methyl-1H-pyrrolo[2,3-b]pyridine (DMP) have been procured from Sigma-Aldrich and used as received, without any further purification.

2.2. Methods

A wide range of analytical techniques was applied, which gave enough information on structural and physicochemical properties of (Z)-3-((2-(2,4-dinitrophenyl)hydrazono)methyl)-4-methyl-1H-pyrrolo[2,3-b]pyridine. The FT-IR spectrum was recorded at room temperature (25 °C) with a Perkin-Elmer FT-IR spectrometer, which enabled the identification of the most important vibrational modes related to functional groups in the molecule. Nuclear magnetic resonance spectra, including ^1H NMR, were recorded on a Bruker AVANCE-III spectrometer. To investigate the electronic transitions of the compound, UV-Vis spectra were recorded on a Perkin-Elmer Lambda 35 spectrophotometer in the 200–800 nm wavelength region with a 1 nm spectral bandwidth. The above measurements gave information about the chromophoric character of the compound. Elemental analysis was performed with a Perkin-Elmer 2400 Series II CHNS/O Analyzer. The elemental percentages observed were in good agreement with the theoretical values calculated, and this confirmed the purity and the elemental accuracy of the targeted compound, DMP.

2.3 Computation

Theoretical calculations were completed using the Gaussian 09 software package [15], with molecular visualization and analysis conducted through the GaussView interface [16]. The DFT (density functional theory) method was employed using the B3LYP/6-311G(d,p) level of theory.

3. Results

3.1 Synthesis of (Z)-3-((2-(2,4-dinitrophenyl)hydrazono)methyl)-4-methyl-1H-pyrrolo[2,3-b]pyridine (DMP),

The Schiff base compound DMP was prepared by the condensation reaction of 4-methyl-1H-pyrrolo[2,3-b]pyridine-3-carbaldehyde (1) with (2,4-dinitrophenyl)hydrazine (2) according to Scheme 1. A typical synthesis involves the dissolution of 0.74 g (3.73 mmol) of (2,4-dinitrophenyl)hydrazine in 20 mL of DMF under constant stirring. To this stirred solution, 0.60 g of the aldehyde (3.74 mmol) was added slowly. This reaction mixture was refluxed for 10 h, during which a pale yellow precipitate appeared gradually when the volume of the solvent reduced to about 10 mL. The reaction was then complete, after which the solid product was separated by filtration and washed thoroughly with 5 mL of cold methanol followed by 10 mL of hexane and finally purified by recrystallization from DMF. The pure compound DMP was collected as yellow crystalline material, dried under vacuum, and yielded 1.10 g (82%) of the expected product.

Elemental Analysis; Elemental analysis of (Z)-3-((2-(2,4-dinitrophenyl)hydrazono)methyl)-4-methyl-1H-pyrrolo[2,3-b]pyridine (DMP) was conducted to confirm its elemental composition and correspondence to the proposed molecular formula, $C_{15}H_{12}N_6O_4$. The calculated elemental percentages for this formula are: carbon (C), 52.94%; hydrogen (H), 3.55%; and nitrogen (N), 24.70%. These values showed excellent correspondence with the experimentally obtained results-C, 52.80%; H, 3.45%; N, 24.60%-thereby confirming the correctness of the proposed structure. The analysis, being carried out in CHN mode on a Perkin-Elmer 2400 Series II CHNS/O Analyzer, did not measure oxygen content directly but obtained it by difference. The calculated proportion of oxygen is in good accord with the molecular formula, further confirming the composition of the compound. This close correspondence between the theoretical and experimental values ensures successful synthesis with high elemental purity of DMP.

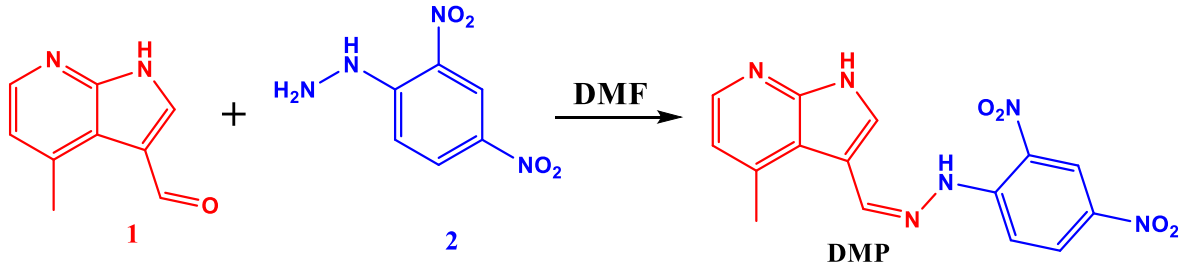

Scheme 1

3.2 NMR Study

The ^1H NMR of DMP acquired in DMSO-d_6 (Figure 2) showed proton signals in agreement with the postulated molecular structure. The azomethine proton (–CH=N–) of the hydrazone linkage, as expected, appeared as a sharp singlet at δ 8.85 ppm due to an isolated environment devoid of coupling interactions [17,18,22]. In the aromatic region, it resonated as a doublet at δ 8.40 ppm which may be assigned to one proton on the pyrrolo[2,3-b]pyridine ring with typical ortho coupling [17,19]. Two additional doublets centered at δ 7.97 ppm and δ 7.22 ppm were assignable to aromatic protons of the 2,4-dinitrophenyl moiety and were consistent with substitution effects and coupling patterns anticipated for electron-deficient aromatic rings.

A singlet at δ 6.60 ppm was assigned to the proton located on the pyrrole ring, reflecting its distinct electronic environment in the fused heterocyclic system [17,20,22]. The hydrazone –NH proton appeared as a small singlet at δ 5.00 ppm, often showing broadening or reduced intensity due to hydrogen bonding and solvent exchange phenomena [17,18]. Finally, a singlet at δ 2.61 ppm corresponded to the methyl group attached at the 4-position of the pyrrolo[2,3-b]pyridine nucleus [17,19]. The integration value for all peaks was as theoretically expected, confirming that the synthesized Schiff base had structural integrity and the formation of the hydrazone linkage was appropriate.

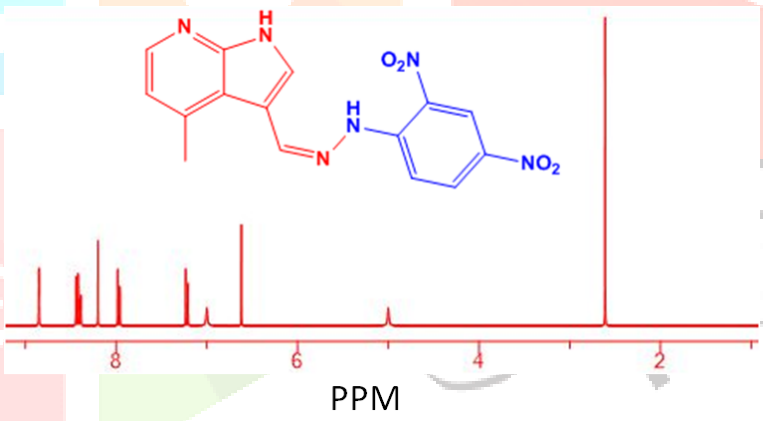

Figure 2 NMR for DMP

3.3 FT-IR Study

The FT-IR spectrum of (Z)-3-((2-(2,4-dinitrophenyl)hydrazono)methyl)-4-methyl-1H-pyrrolo[2,3-b]pyridine (DMP) affords necessary information about the functional groups incorporated into the molecule. A broad absorption band at 3286 cm^{-1} is assigned to the N–H stretching vibration, which indeed reflects the presence of a hydrazone or secondary amine group [21]. The absorption at 3101 cm^{-1} is attributed to aromatic C–H stretching modes, further authenticating the nature of aromaticity in the compound [17,21].

Strong bands at 1619 and 1586 cm^{-1} can be assigned to the C=N and C=C stretching vibrations, respectively, characteristic of the hydrazone (imine) linkage and aromatic ring system. The nitro functionalities are reflected by strong absorptions at 1508, 1330, and 1312 cm^{-1}, which are assigned to asymmetric and symmetric NO_2 stretching modes. Further, aromatic skeletal vibrations were observed at 1447 and 1417 cm^{-1} [17,19,21].

The C–N stretching vibrations of the pyrrolo[2,3-b]pyridine core and hydrazone segment appear at 1261 and 1222 cm^{-1}, respectively. The bands at 1134, 1090, and 1073 cm^{-1} correspond to the in-plane bending of the C–H and C–N bonds. Out-of-plane C–H bending vibrations, characteristic for substituted aromatic systems, are recorded at 922, 894, 834, and 764 cm^{-1} [21,17].

Further characteristic absorptions at 742, 722, 694, 645, and 600 cm^{-1} are indicative of out-of-plane deformation and ring-breathing modes. Bands detected at 523, 507, and 421 cm^{-1} are associated with skeletal deformations involving heavier atoms within the nitro groups and the fused heteroaromatic ring framework [21].

The overall spectral profile clearly establishes the presence of hydrazone, nitroaromatic, and heteroaromatic functionalities fully consistent with the proposed structure for DMP.

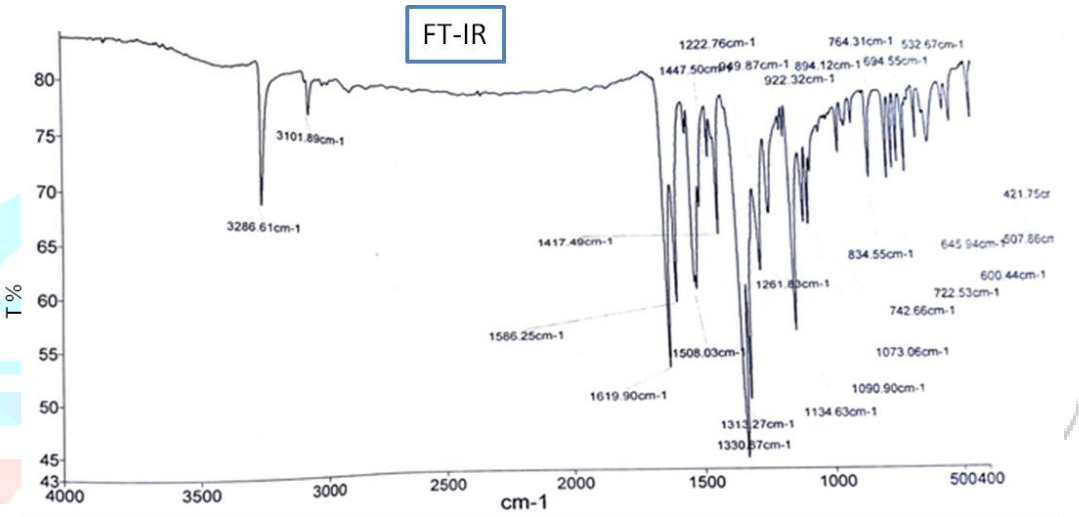

Figure 3 IR for DMP

3.4 UV-Vis Study

Figure 4: The UV–Vis absorption spectrum of (Z)-3-((2-(2,4-dinitrophenyl)hydrazono)methyl)-4-methyl-1H-pyrrolo[2,3-b]pyridine, DMP, exhibits distinct electronic transitions due to its highly conjugated aromatic structure. A strong absorption band appears at 390 nm, assignable to a π→π* transition, due to the extended conjugation between the pyrrolo[2,3-b]pyridine core and the dinitrophenyl-substituted hydrazone segment [17,18]. The intensity of this band reveals a pronounced intramolecular charge transfer ICT process promoted by the electron-rich pyrrolo[2,3-b]pyridine ring and the electrondeficient nitro groups.

A weaker absorption feature at 499 nm is attributed to an n→π* transition, originating from the non-bonding electrons of nitrogen atoms within the hydrazone and nitro functionalities that participate in delocalization over the π-conjugated system. The appearance of this transition at a longer wavelength supports the presence of extended π-conjugation and partial charge separation within the molecule [17–19].

The red shift in the absorption maxima (bathochromic shift) is indicative of strong electron delocalization and increased conjugation across the molecular framework, due to electron-donating and electron-withdrawing substituents acting in concert [17,19,23]. These spectral features confirm the conjugated nature

and electronic complexity of the compound and make DMP a promising candidate for optoelectronic or photochemical applications using intramolecular charge transfer processes.

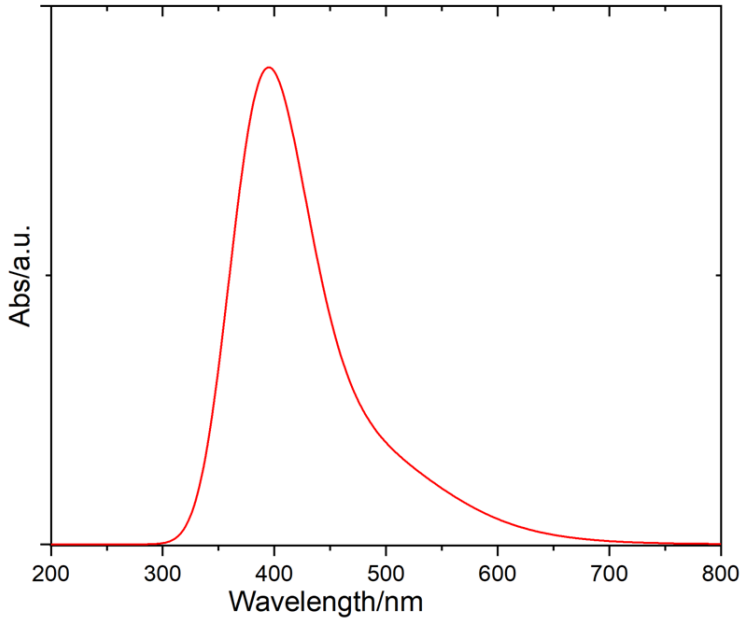

Figure 4 UV-Vis for DMP

3.5 Frontier Molecular Orbital (FMO)

FMO analysis of DMP provides key information on its electronic structure and optical properties [24–26]. According to DFT calculations, HOMO and LUMO energies of DMP were obtained [24,25]. The calculated HOMO and LUMO energies are –6.237 eV and –3.112 eV, respectively, with a gap energy of 3.125 eV. This bandgap energy represents an important parameter for the investigation of molecular reactivity and the probability of electronic transition [24,25,27].

The moderate value of ΔE reveals that DMP maintains a proper balance between stability and reactivity, in agreement with its conjugated structure that favors charge transfer interactions. Molecular-orbital visualization demonstrates that the HOMO is fully delocalized over the whole molecule, while the LUMO density is mainly concentrated over the electron-withdrawing dinitrophenyl-hydrazone segment, indicating an effective intra-molecular charge transfer channel.

Experimentally, the UV–Vis spectrum of DMP exhibits an intense absorption peak at 390 nm, which corresponds to an excitation energy of approximately 3.18 eV as calculated from $E = 1240/\lambda$ [17,28]. The experimental finding is in close proximity to the theoretical HOMO–LUMO gap of 3.125 eV, confirming the strong agreement that exists between DFT predictions and spectroscopic observations.

The good agreement between computational and experimental results confirms the reliability of the DFT method to describe the optoelectronic properties of DMP. These findings enforce its potential applicability in the design of optoelectronic and sensing materials that use intramolecular charge transfer mechanisms. In Figure 5, the HOMO and LUMO orbitals' spatial distributions are presented.

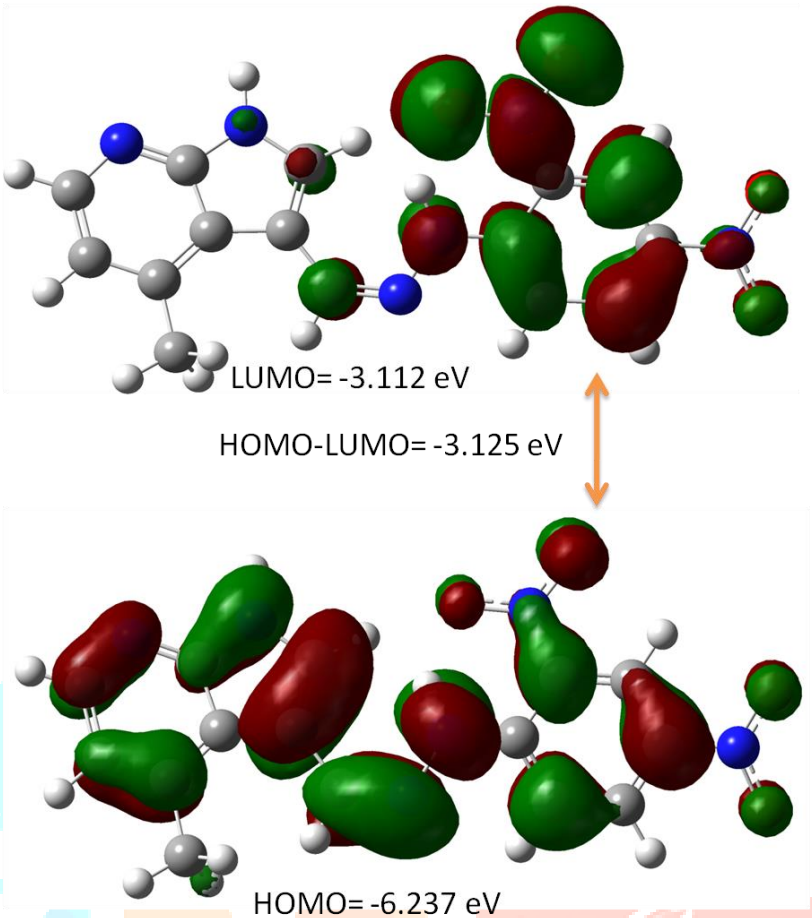

Figure 5 FMO for DMP

3.6 MEP

The MEP map of DMP (Figure 6) was generated within an electrostatic potential range from $–7.13 \times 10^2$ to $+7.13 \times 10^2$ a.u., yielding a clear visualization of charge distribution across the molecular surface. The map reveals that most carbon and hydrogen atoms are enveloped by blue and white regions, corresponding to zones of lower electron density and positive potential, indicating a reduced tendency for these atoms to participate in electrophilic interactions [24–26].

The imine group (C=N) linking the dinitrophenyl and pyrrolopyridine fragments appears within the same white to light-blue regions, indicating moderate electron deficiency. This may also contribute to the stabilization of the molecular conformation and the ease of interaction with nucleophilic species [24,25,29].

In contrast, nitro ($–NO_2$) substituents and nitrogen atoms in the aromatic framework are indicated in red and yellow regions which correspond to higher electron density and negative potential. These sites are likely to be more favorable for electrophilic attack, hydrogen bonding, or possible coordination with metal ions [26,30].

Overall, the MEP surface clearly distinguishes between the electron-rich and electron-poor regions in DMP, thus reflecting its reactive behavior and probable binding sites from both a chemical reactivity and biological standpoint.

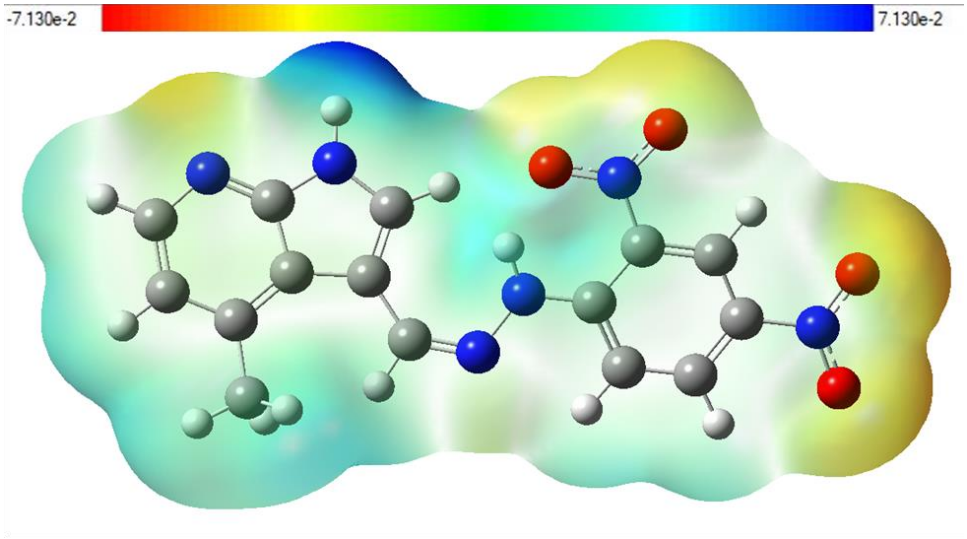

Figure 6 MEP for DMP

4 Conclusion

The synthesis and full characterization of (Z)-3-((2-(2,4-dinitrophenyl)hydrazono)methyl)-4-methyl-1H-pyrrolo[2,3-b]pyridine (DMP) were successfully carried out and verified by elemental analysis and spectroscopic techniques like FT-IR, NMR, and UV–Vis. It was observed that the spectral data confirm the formation of a hydrazone linkage, the presence of aromatic and nitro functionalities, and extended conjugation within the molecule. In addition, theoretical studies by using DFT, including FMO and MEP analyses, supported the experimental results by showing intense intramolecular charge transfer and locating possible reactive sites. The correspondence between experimental results and the computational study ascertains the veracity of the proposed molecular structure and stresses the favorable electronic properties that make DMP a promising molecule for future applications in optoelectronic or molecular sensing areas.

Competing interest

None.

References

[1] Kumar A., Singh A.K., Singh H., Vijayan V., Kumar D., Naik J., et al. (2023). Nitrogen containing heterocycles as anticancer agents: A medicinal chemistry perspective. Pharmaceuticals, 16(2), 299. https://doi.org/10.3390/ph16020299.

[2] Kothawade S.N., Chabukswar A.R., Raut K.G., Sumbe R.B. (2024). Impact and contributions. Paving the path to discoveries and unlocking the secrets of N-heterocycles, 247.

[3] Mir R.H., Mir P.A., Mohi-Ud-Din R., Sabreen S., Maqbool M., Shah A.J., et al. (2022). A comprehensive review on journey of pyrrole scaffold against multiple therapeutic targets. Anti-Cancer Agents in Medicinal Chemistry, 22(19), 3291–3303. https://doi.org/10.2174/1871520622666220617113919.

[4] Petri G.L., Spano V., Spatola R., Holl R., Raimondi M.V., Barraja P., Montalbano A. (2020). Bioactive pyrrole-based compounds with target selectivity. European Journal of Medicinal Chemistry, 208, 112783. https://doi.org/10.1016/j.ejmech.2020.112783.

[5] Yet L. (2018). Privileged structures in drug discovery: Medicinal chemistry and synthesis. John Wiley & Sons.

[6] Singh K., Bhushan B., Mittal N., Kushwaha A., Raikwar C.K., Sharma A.K., et al. (2024). Recent advances in enzyme inhibition: A pharmacological review. Current Enzyme Inhibition, 20(1), 2–19. https://doi.org/10.2174/1573408019666240130151043.

[7] Kogularasu S., Lee Y.Y., Sriram B., Wang S.F., George M., Chang-Chien G.P., Sheu J.K. (2024). Unlocking catalytic potential: Exploring the impact of thermal treatment on enhanced electrocatalysis of nanomaterials. Angewandte Chemie, 136(1), e202311806. https://doi.org/10.1002/ange.202311806.

[8] Pisk J., Đilović I., Hrenar T., Cvijanović D., Pavlović G., Vrdoljak V. (2020). Effective methods for the synthesis of hydrazones, quinazolines, and Schiff bases: Reaction monitoring using a chemometric approach. RSC Advances, 10(63), 38566–38577. https://doi.org/10.1039/D0RA07711J.

[9] Omidi S., Kakanejadifard A. (2020). A review on biological activities of Schiff base, hydrazone, and oxime derivatives of curcumin. RSC Advances, 10(50), 30186–30202. https://doi.org/10.1039/D0RA05337F.

[10] Raczuk E., Dmochowska B., Samaszko-Fiertek J., Madaj J. (2022). Different Schiff bases—Structure, importance and classification. Molecules, 27(3), 787. https://doi.org/10.3390/molecules27030787.

[11] Szatylowicz H., Wieczorkiewicz P.A., Krygowski T.M. (2021). Molecular geometry as a source of electronic structure of π-electron systems and their physicochemical properties. In Aromaticity (pp. 71–99). Elsevier. https://doi.org/10.1016/B978-0-12-822748-1.00005-1.

[12] Tian Y., Cui F., Bian Z., Tao X., Wang H., Zhang N., Zhu G. (2024). Construction of porous aromatic frameworks with specifically designed motifs for charge storage and transport. Accounts of Chemical Research, 57(15), 2130–2143. https://doi.org/10.1021/acs.accounts.4c00213.

[13] Devi M., Kumar P., Singh R., Narayan L., Kumar A., Sindhu J., et al. (2022). A comprehensive review on synthesis, biological profile and photophysical studies of heterocyclic compounds derived from 2,3-diamino-1,4-naphthoquinone. Journal of Molecular Structure, 1269, 133786. https://doi.org/10.1016/j.molstruc.2022.133786.

[14] Zhao Y., Bordwell F.G., Cheng J.P., Wang D. (1997). Equilibrium acidities and homolytic bond dissociation energies (BDEs) of the acidic H−N bonds in hydrazines and hydrazides. Journal of the American Chemical Society, 119(39), 9125–9130. https://doi.org/10.1021/ja970800k.

[15] Frisch M.J., Trucks G.W., Schlegel H.B., Scuseria G.E., Robb M.A., Cheeseman J.R., et al. (2010). Gaussian 09 Revision E.01. Gaussian, Inc., Wallingford, CT.

[16] Dennington R. II, Keith T., Millam J. (2007). GaussView, Version 4.1.2. Semichem Inc., Shawnee Mission, KS.

[17] Pavia D.L., Lampman G.M., Kriz G.S., Vyvyan J.R. (2015). Introduction to Spectroscopy. Cengage Learning.

[18] Pretsch E., Clerc T., Seibl J., Simon W. (2013). Tables of Spectral Data for Structure Determination of Organic Compounds. Springer.

[19] Sharma Y.R. (2007). Elementary Organic Spectroscopy. S. Chand Publishing.

[20] Field L.D., Sternhell S., Kalman J.R. (2013). Organic Structures from Spectra. John Wiley & Sons.

[21] Socrates G. (2004). Infrared and Raman Characteristic Group Frequencies: Tables and Charts. John Wiley & Sons.

[22] Kumar S., Shah P., Tripathi S.K., Khan S.I., Singh I.P. (2022). Synthesis and in vitro evaluation of Hydrazonomethyl-Quinolin–8–ol and Pyrazol–3–yl-Quinolin–8–ol derivatives for antimicrobial and antimalarial potential. Medicinal Chemistry, 18(9), 949–969. https://doi.org/10.2174/1573406418666220607104554.

[23] Liu X., Xu Z., Cole J.M. (2013). Molecular design of UV–vis absorption and emission properties in organic fluorophores: Toward larger bathochromic shifts, enhanced molar extinction coefficients, and greater Stokes shifts. The Journal of Physical Chemistry C, 117(32), 16584–16595. https://doi.org/10.1021/jp4060473.

[24] Al-Ahmary, K. M., Mekheimer, R. A., Al-Enezi, M. S., Hamada, N. M., & Habeeb, M. M. (2018). Synthesis, spectrophotometric characterization and DFT computational study of a novel quinoline derivative, 2-amino-4-(2, 4, 6-trinitrophenylamino)-quinoline-3-carbonitrile. Journal of Molecular Liquids, 249, 501-510.

[25] Ahmad, I., Khan, H., & Serdaroğlu, G. (2023). Physicochemical properties, drug likeness, ADMET, DFT studies, and in vitro antioxidant activity of oxindole derivatives. Computational Biology and Chemistry, 104, 107861.

[26] Raksha, C., Ansiya, N., & Sivan, A. (2025). Integrated DFT, Topological, and ADME Analysis of Isatin-Based Schiff Bases: Synthesis and In Silico Antidiabetic Evaluation. Journal of the Indian Chemical Society, 102105.

[27] Miar M., Shiroudi A., Pourshamsian K., Oliaey A.R., Hatamjafari F. (2021). Theoretical investigations on the HOMO–LUMO gap and global reactivity descriptor studies, natural bond orbital, and nucleus-independent chemical shifts analyses of 3-phenylbenzo[d]thiazole-2(3H)-imine and its para-substituted derivatives: Solvent and substituent effects. Journal of Chemical Research, 45(1–2), 147–158. https://doi.org/10.1177/1747519821993102.

[28] Atkins P.W., De Paula J., Keeler J. (2023). Atkins' Physical Chemistry. Oxford University Press.

[29] Sutradhar T., Misra A. (2021). Theoretical study on the nonlinear optical property of boron nitride nanoclusters functionalized by electron donating and electron accepting groups. The Journal of Physical Chemistry A, 125(12), 2436–2445. https://doi.org/10.1021/acs.jpca.0c11236.

[30] Suresh C.H., Remya G.S., Anjalikrishna P.K. (2022). Molecular electrostatic potential analysis: A powerful tool to interpret and predict chemical reactivity. WIREs Computational Molecular Science, 12(5), e1601. https://doi.org/10.1002/wcms.1601.